RESEARCH ARTICLE

Hidden in plain sight: discovery of sheath-forming, iron-oxidizing *Zetaproteobacteria* at Loihi Seamount, Hawaii, USA

Emily J. Fleming[1], Richard E. Davis[2], Sean M. McAllister[3,], Clara S. Chan[4], Craig L. Moyer[3], Bradley M. Tebo[2] & David Emerson[1]

[1]Bigelow Laboratory for Ocean Sciences, East Boothbay, ME, USA; [2]Department of Environmental and Biomolecular Systems, Oregon Health and Science University, Portland, OR, USA; [3]Department of Biology, Western Washington University, Bellingham, WA, USA and [4]Department of Geological Sciences, University of Delaware, Newark, DE, USA

Correspondence: David Emerson, Bigelow Laboratory for Ocean Sciences, PO Box 380, East Boothbay, ME 04544, USA. Tel.: +1 207 315 2567; fax: +1 207 315 2329; e-mail: demerson@bigelow.org

Present address: Sean M. McAllister, Department of Geological Sciences, University of Delaware, Newark, DE, USA

Received 20 December 2012; revised 28 February 2013; accepted 28 February 2013. Final version published online 15 April 2013.

DOI: 10.1111/1574-6941.12104

Editor: Max Häggblom

Keywords
Leptothrix ochracea; iron-oxidation; *Zetaproteobacteria* FISH probes; Loihi Seamount; convergent evolution; marine iron-mats; deep-sea sampling.

Abstract

Lithotrophic iron-oxidizing bacteria (FeOB) form microbial mats at focused flow or diffuse flow vents in deep-sea hydrothermal systems where Fe(II) is a dominant electron donor. These mats composed of biogenically formed Fe(III)-oxyhydroxides include twisted stalks and tubular sheaths, with sheaths typically composing a minor component of bulk mats. The micron diameter Fe(III)-oxyhydroxide-containing tubular sheaths bear a strong resemblance to sheaths formed by the freshwater FeOB, *Leptothrix ochracea*. We discovered that veil-like surface layers present in iron-mats at the Loihi Seamount were dominated by sheaths (40–60% of total morphotypes present) compared with deeper (> 1 cm) mat samples (0–16% sheath). By light microscopy, these sheaths appeared nearly identical to those of *L. ochracea*. Clone libraries of the SSU rRNA gene from this top layer were dominated by *Zetaproteobacteria*, and lacked phylotypes related to *L. ochracea*. In mats with similar morphologies, terminal-restriction fragment length polymorphism (T-RFLP) data along with quantitative PCR (Q-PCR) analyses using a *Zetaproteobacteria*-specific primer confirmed the presence and abundance of *Zetaproteobacteria*. A *Zetaproteobacteria* fluorescence *in situ* hybridization (FISH) probe hybridized to ensheathed cells (4% of total cells), while a *L. ochracea*-specific probe and a *Betaproteobacteria* probe did not. Together, these results constitute the discovery of a novel group of marine sheath-forming FeOB bearing a striking morphological similarity to *L. ochracea*, but belonging to an entirely different class of *Proteobacteria*.

Introduction

Microbial mats are commonly found in habitats characterized by steep gradients of redox-active substrates. They are highly productive and tend to be stratified into different populations of microorganisms adapted to the specific, yet dynamic physicochemical conditions that exist within the mat (Teske & Stahl, 2002). Deep-sea hydrothermal vents, both at spreading ridge axes and seamounts, offer a case in point by supporting microbial mat communities that take advantage of gradients of inorganic, redox-active compounds in the vent fluids and oxygen in the surrounding ocean. Hydrothermal vent fluids highly enriched in reduced sulfur- or ferrous iron [Fe(II)] compounds often give rise to prolific and diverse microbial mat communities of sulfur-oxidizing or iron-oxidizing bacteria (FeOB), respectively (Ruby *et al.*, 1981; Emerson & Moyer, 2010; Wankel *et al.*, 2011).

Loihi Seamount is an active undersea volcano located at the eastern edge of the Hawaiian hotspot (Garcia *et al.*, 2006). Near the Loihi summit (960 meters below sea level) are a variety of hydrothermal vent sites of low to intermediate temperature (4–60 °C) with both focused and diffuse venting. The vent fluids at Loihi Seamount are highly enriched in Fe(II) as well as CO_2 and are largely devoid of sulfide (Glazer & Rouxel, 2009). The pH of the hydrothermal source fluids can be around 5.5, and plume waters can as low as 7.2 (Garcia *et al.*, 2006).

FEMS MICROBIOLOGY ECOLOGY

Microbial mats at these vents derive their primary energy source from the oxidation of Fe(II), making Loihi a model system for studying communities of marine FeOB. The first convincing evidence for deep-sea communities of FeOB was found at Loihi Seamount (Karl *et al.*, 1989), and it was subsequently shown that FeOB were abundant and formed the mat-like communities responsible for most of the deposition of biogenic Fe(III)-oxyhydroxides (Emerson & Moyer, 2002). The *Zetaproteobacteria*, a novel class of *Proteobacteria*, were discovered at Loihi Seamount and are represented by the novel obligate chemolithotroph *Mariprofundus ferrooxydans* (Emerson *et al.*, 2007). The *Zetaproteobacteria* have subsequently been shown to be an abundant group at other deep-sea and shallow marine hydrothermal systems (Emerson & Moyer, 2010).

One remarkable trait of many FeOB that grow at circumneutral pH is their ability to produce biomineralized extracellular structures such as stalks and sheaths (Emerson *et al.*, 2010). *Mariprofundus ferrooxydans* and related marine strains produce a twisted stalk containing an organic component that controls the deposition of the Fe(III) metabolic byproducts of cell growth (Ghiorse, 1984; Chan *et al.*, 2011). These stalks bear a striking similarity to the structures produced by the freshwater FeOB *Gallionella ferruginea* (Comolli *et al.*, 2011). Until recently, this led to the assumption that the stalk-like structures that are commonly associated with flocculent Fe(III)-oxyhydroxide deposits at iron-rich deep-sea vents were formed by *Gallionella*. However, phylogenetic analysis has shown that *Mariprofundus* and *Gallionella* are distantly related (Emerson *et al.*, 2007) and share few highly homologous functional genes (Singer *et al.*, 2011). Furthermore, a number of cultivation-independent studies of marine iron-mats (Davis & Moyer, 2008; Hodges & Olson, 2009; Kato *et al.*, 2009; Rassa *et al.*, 2009; Forget *et al.*, 2010; Handley *et al.*, 2010; McAllister *et al.*, 2011; Meyer-Dombard *et al.*, 2012) found evidence for *Zetaproteobacteria* related to *M. ferrooxydans,* but not for bacteria related to *Gallionella* species. Thus, it appears that the morphological, ecological, and physiological commonalities between *Mariprofundus* and *Gallionella* are not due to a close genetic relatedness but may be the result of convergent evolution.

Another FeOB morphotype observed in Loihi Seamount iron-mats is filamentous cells encased in a robust sheath composed primarily of Fe(III)-oxyhydroxides (Emerson & Moyer, 2002, 2010). Morphologically, these structures bear striking resemblance to a commonly observed freshwater FeOB morphotype that of *Leptothrix ochracea* (Fleming *et al.*, 2011). At Loihi Seamount, these tubular structures have remained a mystery because they have only been observed sporadically. Thus, it has not been possible to associate them with any specific vent site or condition. Furthermore, there are few reported observations of such structures in other marine iron-mats (Hodges & Olson, 2009; Li *et al.*, 2012).

In freshwater iron-mat communities, *L. ochracea* is easily recognizable due to its copious production of hollow, tubular Fe(III)-oxyhydroxide-encrusted sheaths mostly devoid of cells; even in the most actively growing mats, only 10% of the sheaths contain cells (Emerson & Revsbech, 1994; Fleming *et al.*, 2011). Only recently, cultivation-independent analysis has shown that *L. ochracea* is a member of the *Betaproteobacteria*, related to other sheath-forming heterotrophic *Leptothrix* spp., and *Sphaerotilus* spp. (Fleming *et al.*, 2011). Despite *L. ochracea's* relationship to these heterotrophic sheath-formers, its physiology remains unclear; it cannot be enriched on media that support growth of *Sphaerotilus* spp. or other *Leptothrix* spp., and, unlike these organisms, it has an absolute requirement for Fe(II). This has led to speculation that it may be a lithotroph that utilizes Fe(II) as an energy source (Emerson *et al.*, 2010).

The role of these *Leptothrix*-like sheath-forming bacteria in marine systems is even less understood. Cultivation-independent studies of marine iron-mat communities have not reported the presence of SSU rRNA gene sequences related to *L. ochracea*, or other iron-oxidizing *Betaproteobacteria*. However, because the sheaths are infrequently observed, and the cells are even rarer, it is possible they have simply gone undetected. In a recent expedition to the iron-mats at Loihi Seamount, we were able to collect a thin veil-like layer on the surface of active iron-mats, which was highly enriched in sheath structures. Our goal was to determine whether the sheath producing bacteria found at Loihi were closely related to sheath producing *L. ochracea* found in freshwater habitats.

Materials and Methods

Site/sample collection

The description of microbial mat ecosystems at Loihi Seamount, including ecological and biomineralogical analyses, has been previously published (Glazer & Rouxel, 2009; Rassa *et al.*, 2009; Emerson & Moyer, 2010; Edwards *et al.*, 2011; Toner *et al.*, 2012). For this study, we focused on collecting thin, cream-colored veil-like mats (see Fig. 1) using a custom-designed biomat syringe (BS) sampler that could be operated with the manipulator arms of the remotely operated vehicle (ROV), JASON II. A 100 cc plastic syringe was modified by attaching metal rods to both sides of the barrel, a lanyard onto the plunger, and a short length (~5 cm) of double-walled tygon tubing to the syringe tip. The manipulator arm gripped the syringe and

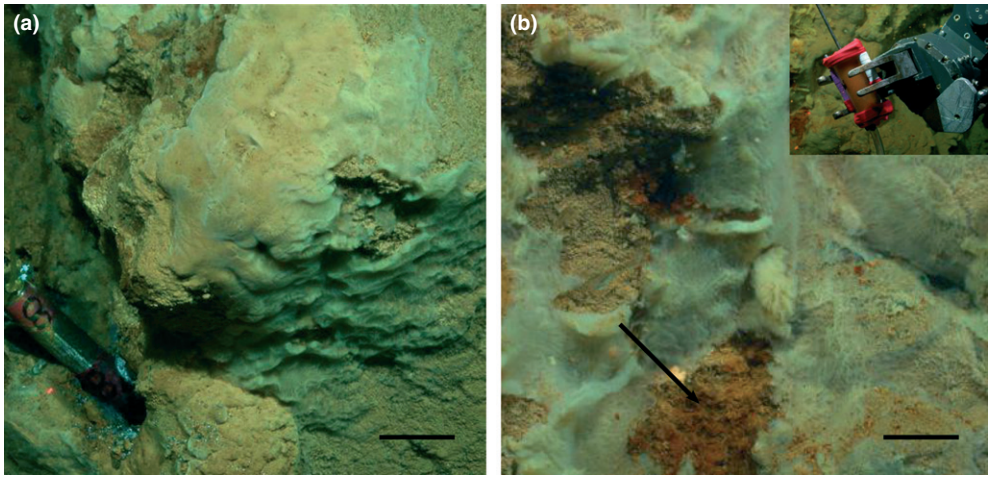

Fig. 1. Images of the filmy layer on top of the iron-mats. (a), An undisturbed surficial mat close to a vent at Marker 31 Upper Hiolo North, (the stainless steel canister #8) is a long-term temperature probe that is placed in the vent orifice; (b), A close-up image of the surficial layer at Ku'kulu, the arrow denotes an area where a syringe sample was taken, exposing the darker more crusty iron-mat beneath. The inset shows a syringe sampler after sampling. Scale bars are 10 cm for a and 2 cm for b.

moved it until the tip was just touching the surface of a mat; finally, the plunger was retracted by pulling the lanyard with the other manipulator arm resulting in collection of surficial mat layers. As soon as the BS samplers were returned to the surface, they were subsampled and processed as follows: (1) approximately 1 mL was fixed in glutaraldehyde (2.5% final conc.) and stored at 4 °C for morphological analysis; (2) another 1 mL was fixed in paraformaldyde for 1.5 h, washed with PBS, resuspended in 1 : 1 PBS: ethanol, and stored at −20 °C for fluorescence *in situ* hybridization (FISH), and (3) the remainder was stored at -80 ° C for DNA analysis.

Samples were collected from the iron-mats surrounding several active vents on Loihi Seamount (including Marker 39, upper Marker 31, Marker 57, and a newly discovered vent site, Ku'kulu N 18° 54.326364′ W 155° 15.423078′). These sites are present on the summit of the Loihi seamount in Pele's Pit near the Hiolo ridge (Marker 39 and Marker 31), the southern vents (Marker 57) or the southern wall (Ku'kulu). Samples were collected from different mat morphologies (veil-like, lobate or streamers) at Marker 57, Marker 39,and Marker 31, or from the upper layer (BS samples), or deeper in the mats (bulk mat suction samples; Marker 39 and Marker 31). These were used to compare the microbial community composition (clone libraries and T-RFLP), the Fe(III)-oxyhydrioxide morphology (microscopy), the number of *Zetaproteobacteria* (qPCR), the number of sheathed *Zetaproteobacteria* (qPCR and FISH).

Morphological analysis

Light microscope analysis of Fe(III)-oxyhydroxide structures was performed by spreading 10 μL of a artificial seawater diluted mat sample (typically 1 : 50 dilution) on agarose-coated glass slides etched with a 10 mm diameter ring (Electron Microscopy Sciences, Hatfield, PA) and allowed to air dry, as described previously (Emerson & Moyer, 2002). Slides were visualized on an Olympus BX60, and images were captured using a QICAM FAST CCD camera and QCapturePro software (QImaging, Surrey, BC, Canada). Images were imported into ImageJ (Rasband, 2004), and morphological structures were traced using a Wacom Intous4 PenTab drawing tablet (Saitama, Japan). The total area of each structure (sheath, stalk, and particulate) was then used to calculate the percent of each structural type at each sampling site.

Scanning electron microscopy (SEM)

Samples were filtered onto 0.2 μm-pore size polycarbonate filters (Millipore, Billerica, MA), rinsed with ultrapure water, and air-dried. Filters were mounted onto aluminum stubs with carbon tape and coated with Au/Pd in a Denton Bench Top Turbo III sputter coater. The samples were imaged at the Delaware Biotechnology Institute Bioimaging Facility using a Hitachi S-4700 field emission scanning electron microscope (FE-SEM, Hitachi, Tokyo, Japan) with an accelerating voltage of 3.0 kV. Energy dispersive X-ray spectroscopy (EDX) was conducted at 15 kV, using an Oxford Instruments INCAx-act silicon drift detector.

Genomic DNA preparation

Genomic DNA (gDNA) was extracted from frozen samples using the Fast DNA SPIN Kit for Soil (Qbiogene, Carlsbad,

CA) according to the manufacturer's protocol with the modification that gDNA was eluted into 10 mM Tris at pH 8 (Tris buffer). To optimize the cellular lysis step, a FastPrep Instrument (Qbiogene) was used at an indexed speed of 5.5 for 30 s. The purity and concentration of gDNA were determined with a NanoDrop ND-1000 spectrophotometer. All gDNA was then diluted for downstream analysis to ~10 ng μL^{-1} using Tris buffer.

PCR amplification and cleanup of the SSU rRNA gene

Bacterial small-subunit ribosomal RNA (SSU rRNA) genes were amplified from the purified gDNA using the 68F forward primer and the 1492R reverse primer (Described in Table S1); (manufactured by Glen Research, Sterling, VA). Replicate PCRs were performed using reagents and conditions as previously reported (McAllister *et al.*, 2011). Amplicon size was confirmed by 1% agarose gel electrophoresis. Replicate PCRs were pooled, concentrated, and desalted with a VWR modified PES 30K centrifugal filter (VWR International, Radnor, PA). The desalted amplicons were eluted in Tris buffer.

Terminal-restriction fragment length polymorphism (T-RFLP)

Three replicate PCR reactions were performed and cleaned up as described previously (Davis & Moyer, 2008), with the modification that the forward primer was 5′ end-labeled with a 6-FAM fluorescent dye. Pooled and concentrated amplicons were diluted to 120 μL in Tris buffer and split between eight restriction enzyme treatments using the following tetrameric restriction endonucleases: AluI, BstUI, HaeIII, HhaI, HinfI, MboI, MspI, and RsaI (New England BioLabs, Ipswich, MA). Restriction digests were carried out in NEB buffer 4 at 37 °C for all enzymes except BstUI, which was run at 60 °C. Reactions were desalted using Sephadex superfine G-75 (Amersham Biosciences, Uppsala, Sweden) and dried down. Reactions were resuspended in 15 μL of a 1 : 29 solution of LIZ-500 internal size standard in formamide, denatured at 95 °C for 5 min, and separated by capillary electrophoresis using an ABI 3130xl genetic analyzer with a 50-cm capillary array and POP-6 polymer (Life Technologies, Carlsbad, CA). Electropherograms were imported into BioNumerics (Applied Maths, Sint-Martens-Latem, Belgium) and sized against the LIZ-500 internal size standard. Community fingerprints were compared as described previously (Rassa *et al.*, 2009), using average Pearson product moment correlation and unweighed pair group method with arithmetic mean (UPGMA) cluster analysis on all eight restriction digests. This method compares the relative fluorescent proportions of each electropherogram. Cophenetic correlation coefficient values were calculated as a metric to assess the robustness of dendrogram groupings. Analysis was confined to fragment sizes of between 50 and 500 base pairs.

SSU rRNA gene clone library construction

Five replicate PCR reactions for SSU rRNA were performed and cleaned up as described previously (Davis & Moyer, 2008). The desalted amplicons were then cloned with a CloneJET PCR Cloning Kit following the manufacturer's instructions (Fermentas Inc, Glen Burnie, MD). All putative clones were streaked for isolation, and the inserts assayed for correct size using PCR with pJET1.2 forward and reverse primers. Clones were then grown up in Terrific Broth (Tartof & Hobbs, 1987) with 100 μg mL^{-1} amplicillin and sent for sequencing at Beckman Coulter Genomics (Danvers, MA).

Initial operational taxonomic unit (OTU) composition for each clone library was determined based on reads from the 5′ end of the SSU rRNA gene. Sequences were aligned to the ARB-SILVA database using the SINA Webaligner function (Pruesse *et al.*, 2007) and masked so that only unambiguously aligned sequence data would be used for phylogenetic/taxonomic analyses. OTUs were defined based on a minimum similarity of 97%. At least one clone from each OTU was randomly selected for full-length sequencing. Plasmids for these clones were isolated and purified using standard alkaline lysis and sequenced on an ABI 3130xl genetic analyzer using internal sequencing primers (Lane, 1991). SSU rRNA gene sequences were contiguously assembled using BioNumerics (Applied Maths) and checked for chimeras using Pintail (Ashelford *et al.*, 2005) and Mallard (Ashelford *et al.*, 2006).

Nucleotide sequence accession numbers

The SSU rRNA gene sequences from this study have been submitted to GenBank and were assigned accession numbers JQ287646 through JQ287657 and JX468894.

Zetaproteobacteria quantitative PCR primer and FISH probe design

All full-length sequences in the NCBI database belonging to the *Zetaproteobacteria* were aligned using the SILVA SINA web aligner (Pruesse *et al.*, 2007) and imported into the SILVA 102 NR database managed using the ARB sequence program (Ludwig *et al.*, 2004). The PROBE MATCH tool was used to build the quantitative PCR (Q-PCR) primers specific for the *Zetaproteobacteria*, Zeta537F and Zeta671R, and the FISH probe, Zeta674

(Table S1). The Zeta 674 probe was located in a relatively inaccessible region of the SSU rRNA; therefore, it was necessary to use additional unlabeled helper probes (ZetaH699, ZetaH722 and ZetaH710; Table S1) that flanked the Zeta674 target sequence as similarly detailed in Fuchs *et al.*, 2000. These helper probes significantly improved hybridization and visualization of the Zeta 674 probe.

The total bacterial SSU rRNA copy number was quantified with general bacteria primers Bact533F and Bact684R for Q-PCR, and the EUB338 and NON338 FISH probes were used for positive and negative controls for FISH (Amann *et al.*, 1990 and Wallner *et al.*, 1993).

Quantitative PCR optimization and analysis

The Q-PCR primers were optimized for efficiency and specificity using a StepOnePlus real-time PCR system (Life Technologies) and DyNAmo Flash SYBR green PCR master mix (ThermoFisher Scientific, Waltham, MA). The Zeta 537F and Zeta 671R primer set were designed to exclusively amplify all of the known *Zetaproteobacteria* sequences in the ARB SILVA release 102 Ref database. Furthermore, the primer pair also included all *Zetaproteobacteria* sequences found in the clone libraries prepared for this study. Details, including use of controls, are described in the Data S1. Copy numbers of total bacteria and *Zetaproteobacteria* were quantified in 1 ng of gDNA using absolute quantitation against linearized plasmids by digestion with the restriction enzyme NotI (New England Biolabs). Proportions of *Zetaproteobacteria* were calculated by dividing the total copy number of *Zetaproteobacteria* by the copy numbers found using the general bacteria primer set. All reactions were performed in triplicate and checked for specificity with a melting curve.

Catalyzed reporter deposition fluorescence *in situ* hybridization (CARD-FISH)

Paraformaldehyde preserved samples were spread on ClearCell (ThermoScientific, Waltham, MA) slides, air-dried, and then dipped in 0.1% gelatin (Type B; Sigma-Aldrich Saint Louis, MO) or 0.5% low melting point agarose (EMD, Gibbstown, NJ) for < 5 s. Probes were manufactured by biomers.net GmbH (Ulm, Germany) with an attached horseradish peroxidase (HRP) for use with fluorescent labeled tyramides for CARD-FISH. CARD-FISH was then performed as described in Pernthaler *et al.* (2002), with the Invitrogen-Molecular Probes TSA #42 kit (Carlsbad, CA), with several modifications that are detailed in the Data S1. Prior to visualization, Syto13 (in 5 mM DMSO, Invitrogen-Molecular Probes) was added to each sample. Slides were visualized both with fluorescence microscopy (Olympus BX60) and with confocal microscopy (Zeiss LSM700, Jena, Germany). All images were then processed using ImageJ (Rasband, 2004).

Optimization of FISH probes

The formamide concentration was used to optimize the binding stringency of the probe so that it would distinguish between a single base pair mismatch (Details in Data S1). The marine iron-oxidizing *Zetaproteobacteria* isolate, *Mariprofundus* sp. GSB-2 (McBeth *et al.*, 2011) was an exact sequence match to the Zeta674 FISH probe, and the freshwater heterotroph *Ottowia thiooxydans* (Spring *et al.*, 2004) contained a single base pair mismatch. At 20% formamide, the Zeta674 FISH probe could discriminate between GSB-2 and *O. thiooxydans*. All subsequent hybridizations were performed at 20% formamide and included both control strains.

Results

Structure and composition of mat surface layer

Our curiosity was spurred by the observation of microbial mats with a cream-colored, surface biofilm with a veil-like appearance during a previous Loihi cruise (Iron Microbial Observatories at Loihi Volcano, FeMO 2007 & 2008 and Emerson & Moyer, 2002). These surficial films occurred in proximity to some vent orifices and were adjacent to, instead of directly in the vent flow. The bulk sampling methods that were used previously to collect the mats would have diluted these surface films with the

Table 1. Percentage of sheath morphotypes in different Loihi Seamount mat samples comparing BS sampler and bulk mat suction sampler

Morphotype	Ku'kulu Syringe sampler (BS8)	Hiolo North (Marker 39)		Upper Hiolo North (Marker 31)	
		Syringe sampler (BS4)	Bulk mat suction sampler	Syringe sampler (BS7)	Bulk mat suction sampler
Sheath	41%	58%	16%	61%	0%
Stalk	36	12	55	13	37
Particulate*	23	31	30	26	63

*Includes both biologically and abiotically produced Fe(III)-oxyhydroxide minerals.

more condensed, thicker underlying iron-mat. This led to development of the BS sampler, which can selectively acquire surface layers < 0.5 cm thick (Fig. 1). Shipboard light microscopic analysis of BS samples of the cream-colored biofilm immediately revealed that it was highly enriched in iron-encrusted sheaths, reminiscent of the freshwater *L. ochracea*. Subsequent quantitative morphological analysis confirmed that sheaths were much more abundant in these veil-like surface layers than in the underlaying bulk mat (Table 1).

Light microscopic analysis confirmed the morphological similarity between marine and freshwater sheathed FeOB (Fig. 2). The long tubular sheaths from Loihi Seamount had the same general appearance as sheaths from a freshwater wetland in Maine (Fleming *et al.*, 2011). They were of similar widths (~1 μm in diameter) and 100 s of μm long. Like the freshwater sheaths, the sheaths formed at Loihi had few cells inside. The marine sheaths were observed under light microscopy to dissolve quickly when treated with oxalic acid (~0.25 M, final concentration; results not shown). This indicates that their structural integrity was dependent on the presence of Fe(III)-oxyhydroxides.

The tubular nature of the marine and freshwater sheaths was also visible in the samples analyzed by SEM (Fig. 2b and d). Both types of sheaths broke easily (a characteristic also observed in wet mounts by light microscopy), explaining the short fragments in the SEM images. A significant percentage of freshwater sheaths were collapsed in SEM images, whereas the marine sheaths were not (Fig. 2b and d); this indicates that the marine sheaths were more robust, likely due to heavier mineralization. The freshwater *L. ochracea* sheaths were collected from mats that had formed overnight; we do not know the age of the Loihi Seamount sheaths, although it is unlikely they were more than days or weeks old. The sheath fibril ultrastructure visible in the SEM varied between the two sheath types, the marine sheaths contained thicker individual fibrils arranged into a more open, porous texture, while the thinner, delicate freshwater sheath fibrils formed a smoother solid surface. EDX spectra show that both marine and freshwater sheaths are rich in Fe and O (Fig. S1), an observation consistent with a composition of Fe(III)-oxyhydroxides and with the reports of others (James *et al.*, 2012).

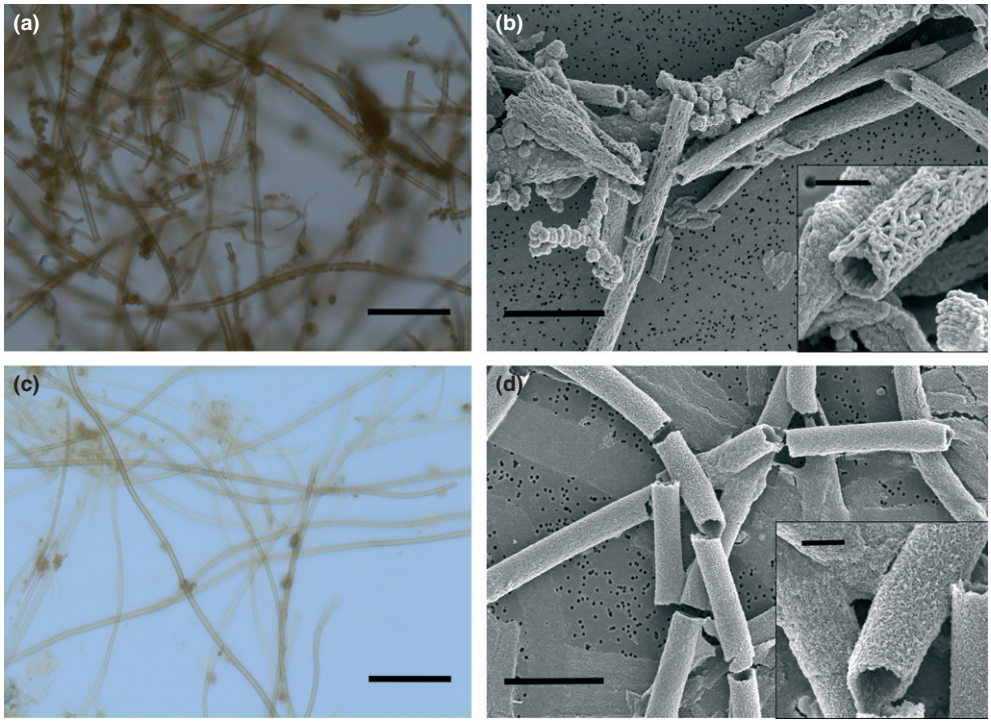

Fig. 2. Micrographs showing the overall similarity between representative samples of marine and freshwater sheaths (1). The top panels show, (a) a light micrograph of a sample taken with a syringe sampler (Marker 39 BS4), and (b) an SEM image of this sample that shows the fine structure of the sheaths. The lower panels show a sample taken from a local freshwater iron-seep in Maine morphologically dominated by *Leptothrix ochracea*; (c), a light micrograph; (d) an SEM image showing fine structure of the sheaths; note, some of the sheaths have collapsed (2). Scale bars for a and c are 15 μm, b and d 5 μm with panels insets 1 μm. Stalks (3) and particulates (4) are also denoted with numbered arrows.

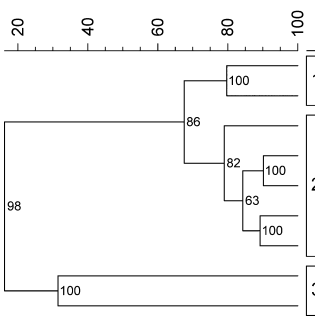

BS Sample	Sampling Site	% ζ	Temp.	Description/ Observed Morphology
J2-476_BS6	Mkr #39 Hiolo North	41.8	42.6	Crumble/lobate structure
J2-479_BS5	Mkr #57 Pohaku	79.3	27.8	Curds/lobate structure
J2-483_BS8	Ku'kulu South Base	18.4	46.6	Veil-like
J2-481_BS4*	Mkr #39 Hiolo North	23.5	42.6	Veil-like
J2-482_BS7*	Upper Mkr #31 Hiolo North	21.2	40.6	Veil-like
J2-482_BS4	Upper Mkr #31 Hiolo North	19.2	40.6	Veil-like
J2-476_BS4	Mkr #39 Hiolo North	25.2	42.6	Veil-like
J2-476_BS1	Mkr #39 Hiolo North	16.5	42.6	Streamers at Vent source
J2-482_BS8	Upper Mkr #31 Hiolo North	9.6	40.6	Streamers at Vent source

Fig. 3. Cluster analysis of bacterial T-RFLP fingerprints from 9 BS samples taken from upper portion of the mat at various sites at Loihi Seamount. Samples with differing observed mat morphology group into three clusters (indicated). Q-PCR data, percentages generated using *Zetaproteobacteria*-specific and bacterial primers, are also indicated. Temperature upon collection was approximately the same for each sample. Samples highlighted with an asterisk were chosen for clone library analysis. Numbers at nodes are cophenetic correlation coefficients.

Molecular analysis of mats

Each mat morphology had a different microbial community composition that was evident in the T-RFLP analysis (Fig. 3). In addition to the cream-colored veil-like mats, samples were also collected from surface mats consisting of condensed lobate chunky/caked structures and from streamers at vent orifices. Each of these mat morphologies grouped within one of three distinct clusters when compared by cluster analysis (Fig. 3). BS samples from the Group 1 lobate structures had a higher percentage of *Zetaproteobacteria* in the bacterial community than the other two groups, as determined by Q-PCR analysis (Fig. 3, Column 4). The Group 3 T-RFLP patterns were associated with the streamers located in vent orifices and had low percentages of *Zetaproteobacteria*. Sheaths were not observed in these samples. The samples collected for the focus of this study (i.e. cream-colored veils, dominated by sheaths) clustered into Group 2. The sheath-dominated Group 2 samples had on average 21.5% average *Zetaproteobacteria*, and two of these samples were selected for further analysis with SSU rRNA gene clone libraries.

A total of 128 clones of the SSU rRNA gene were recovered from Marker 39 (BS4; $n = 60$ clones) and Upper Marker 31 (BS7; $n = 68$ clones). Most of the clones (95% at Marker 39 and 81% at Marker 31) belonged to the *Proteobacteria*, with the majority of the clones (75% of both libraries) belonging to either the order *Chromatiales* (in the class *Gammaproteobacteria*), or the class *Zetaproteobacteria* (Figs 4 and 5). The presence of the *Zetaproteobacteria* (37% at Marker 39 and 29% at Marker 31) was expected based on previous analyses of bulk mat samples from these same sites (Rassa *et al.*, 2009; McAllister *et al.*, 2011). The abundance of the *Chromatiales* in the surface layer clone libraries was substantially greater than the abundance found in bulk mat,

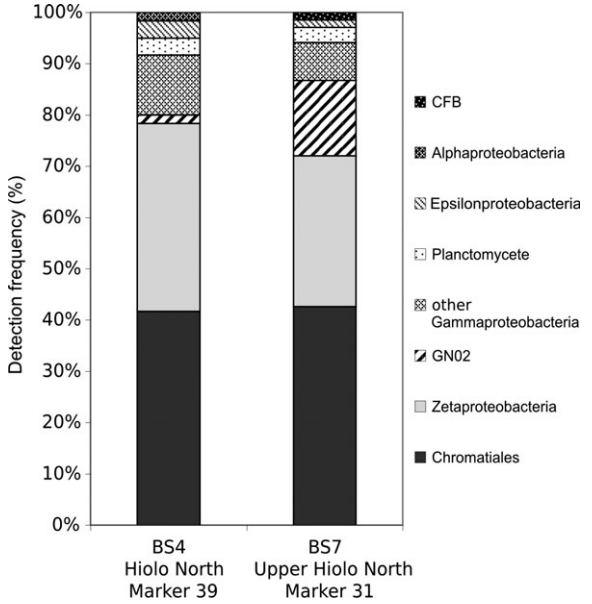

Fig. 4. Stacked bar graph showing the detection frequency of clones obtained from two syringe samples taken from upper layers of mat at Markers 39 and 31. Classification was determined using the RDP classification hierarchy at 80% confidence.

where these phylotypes are present, but not common (data not shown). While the relative abundance of *Chromatiales* was high in these surficial mats, the diversity of OTUs was quite low. Only one distinct *Chromatiales* OTU was recovered from each library.

Overall, the two communities resembled one another; 19 OTUs from the Marker 39 library and 18 OTUs from the Marker 31 library had very similar OTU assignments (Table 2), as was predicted by the T-RFLP analysis. The largest observed difference was that the Marker 31 library had 10 clones (14.7% of the library) that belonged to the candidate division or phylum GN02, while only one clone

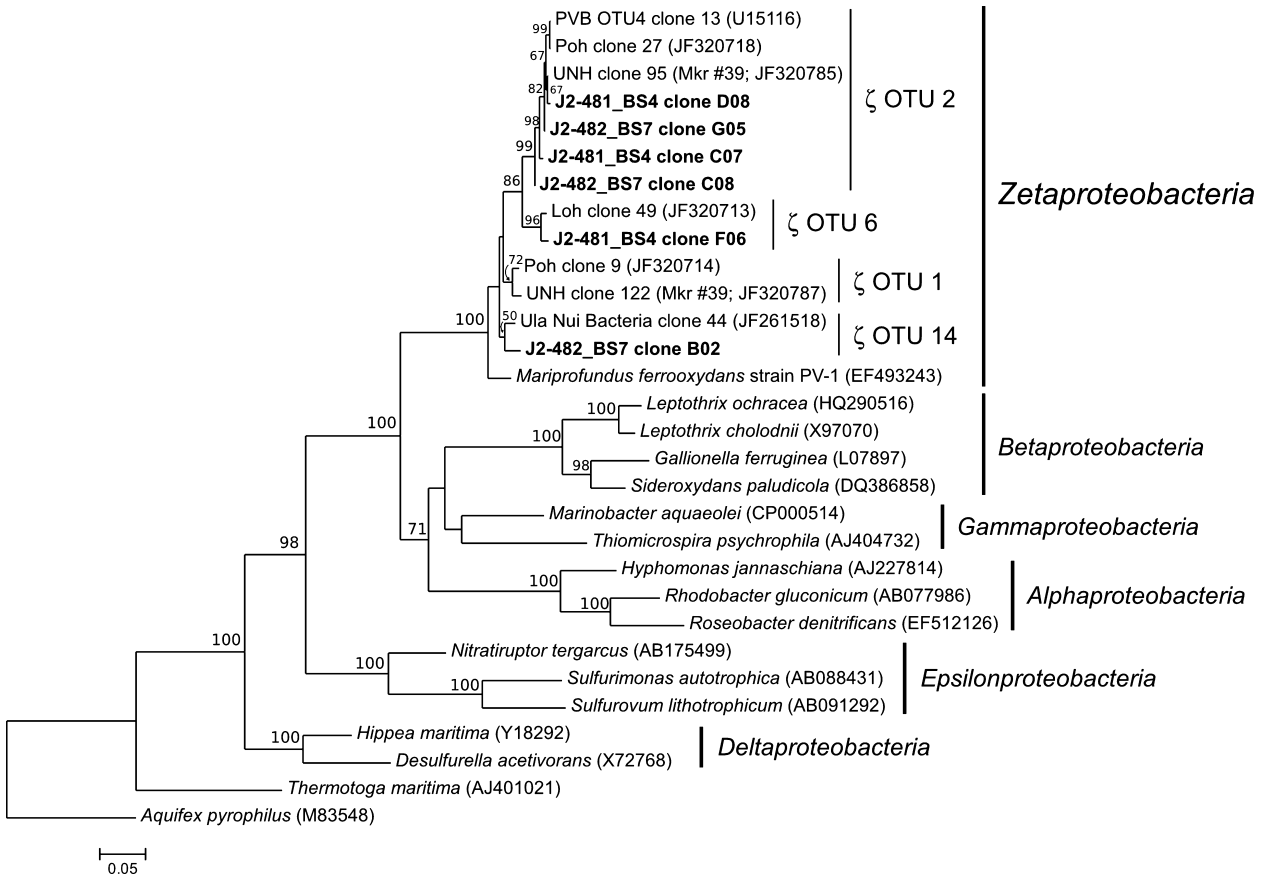

Fig. 5. Maximum likelihood phylogenetic tree showing the evolutionary placement of the six full-length *Zetaproteobacteria* sequences representing five OTUs detected from the BS sampler clone libraries constructed for this study. Additional *Zetaproteobacteria* sequences are provided to anchor these novel sequences within the previously described *Zetaproteobacteria* biodiversity hierarchy, indicated by 'ζ OTU n' (McAllister *et al.*, 2011). Accession numbers for published sequences are shown in parentheses. Only bootstrap values above 50 are shown. Scale bar represents five nucleotide substitutions per 100 positions.

(1.7% of the library) of this group was found at Marker 39.

FISH

FISH analysis revealed that all sheath-encased filaments of cells bound to the Zeta673 probe, confirming that these cells were indeed *Zetaproteobacteria* (Fig. 6). Probes specific for the *Betaproteobacteria* (BET42a) and for *L. ochracea* (Lepto175) did not bind to the sheathed cells (or the nonsheathed cells) in Loihi Seamount samples but did bind sheathed cells in the freshwater samples (data not shown). Additionally, the Zeta674 probe did not bind to sheathed cells from freshwater samples enriched in *L. ochracea* (data not shown; McBeth *et al.*, 2013). The Zeta674 probe also bound to a majority of the nonsheathed cells; specifically, 87% of the cells from Marker 31 and 54% of the cells from Marker 39. The great majority of these cells were attached to stalks, particulate Fe(III)-oxyhydroxides or on the outside of empty sheaths. Only 4–5% of the cells were actually encased in sheaths, that is, most sheaths were empty. When quantified by FISH, the *Zetaproteobacteria* percentages were greater than when quantified by SSU rRNA gene copy number or the number of clones (Table 3). While nonspecific binding of FISH probes could artificially increase cell percentages, this effect is likely minimal due to the discriminatory nature of the Zeta674 probe between controls with a single basepair mismatch.

Discussion

Microbial mat communities in terrestrial and shallow marine ecosystems often have well-defined structures created by the presence of different microbial populations that are adapted to specific redox conditions or light levels that exist in the mat (Teske & Stahl, 2002). While it is known that different mineralogical layers within high

Table 2. Clone library information for OTUs with two or more clones

Clone library	OTU	Sequenced clone no.	No. of clones (% of library)	Phylogenetic grouping*
Hiolo North (Marker 39) BS4	1	C08 & C10	24 (40.0)	*Chromatiales*
	2	C07 & D08	15 (25.0)	*Zetaproteobacteria*
	3	F06	3 (5.0)	*Zetaproteobacteria*
	4	A07	2 (3.3)	Unclassified *Gammaproteobacteria*
	5	C06	2 (3.3)	*Colwelliaceae*
Upper Hiolo North (Marker 31) BS7	1	F08 & H12	27 (39.7)	*Chromatiales*
	2	G05	12 (17.6)	*Zetaproteobacteria*
	3	G06	10 (14.7)	GN02
	4	B02	4 (5.9)	*Zetaproteobacteria*
	5	C08	2 (2.9)	*Zetaproteobacteria*

*Classification was determined using the RDP classification hierarchy at 80% confidence.

temperature hydrothermal vent chimneys can have discrete populations (see for example, Kormas *et al.*, 2006), direct evidence for structured microbial mat communities at deep-sea hydrothermal vents is rare. In this study, we found clear evidence for morphologically and phylogenetically distinct populations using an *in situ* sampling device capable of acquiring thin, visually distinctive layers within an iron-rich microbial mat formed in response to opposing redox gradients of Fe(II) and O_2.

The cream-colored veil-like biofilms observed in some of the iron-mats at Loihi Seamount are morphologically dominated by sheath-forming FeOB. The fact that we did not find these organisms deeper in the same mats, or at sites where the veil-like layer was not present, helps to explain why marine sheath-forming FeOB have only been observed sporadically (Emerson & Moyer, 2010). Perhaps, more surprising is the discovery that the sheath-forming bacteria at Loihi Seamount belong to the *Zetaproteobacteria* and are not related to *L. ochracea,* despite sharing similar lifestyles and a remarkable morphological resemblance.

Observations made during this study confirm that like *L. ochracea*, the marine sheath-formers produce largely empty long, straight tubular sheaths that become mineralized with Fe(III)-oxyhydroxides. This morphology is consistent with a lifestyle for bacteria that utilize Fe(II) as an energy source. In terms of thermodynamic yield, Fe(II) is a poor energy source; therefore, an iron-oxidizing lithotroph needs to oxidize large amounts of Fe(II) to produce biomass (Neubauer *et al.*, 2002). For these sheath-forming FeOB, that translates into production of large amounts of sheath per cell, which helps to explain why even in actively growing populations, most of the sheaths are empty. The massive iron-oxidation and sheath production aids in the accumulation of substantial mats (Fig. 1). Similar to freshwater systems, ensheathed cells are most abundant in the outer edges of the mat (Emerson & Revsbech, 1994). This is in contrast to nonsheathed FeOB that are present throughout the mat, suggesting an ecologically different niche.

Betaproteobacteria, which include the freshwater FeOB *Gallionellales* and *Leptothrix* spp., were conspicuously absent in these Loihi iron-mats, as observed by FISH as well as SSU rRNA gene clone libraries. Among the *Zetaproteobacteria* OTUs that were fully sequenced, almost all of the clones (29 of 36 or 81%) clustered within the previously described *Zetaproteobacteria* OTU 2 (Figs 4 and 5; McAllister *et al.*, 2011). The *Zetaproteobaceteria* OTU 2 cluster is one of the most commonly found OTUs at Loihi Seamount and appears to be quite a cosmopolitan group with other representatives coming from iron-rich vent sites in the Eastern and Western Pacific (McAllister *et al.*, 2011). This group also includes clone PVB_13, from the Loihi Seamount, which with other sequences helped form the first identified *Zetaproteobacteria* OTU (Moyer *et al.*, 1995).

In all, 12 different *Zetaproteobacteria* OTUs have been identified at Loihi Seamount. In this study, one *Zetaproteobacteria* OTU represented the majority of the *Zetaproteobacteria* sequences, and the diversity within the veil-like surface mat layer was lower than the overall diversity of *Zetaproteobacteria* at Loihi Seamount (McAllister *et al.*, 2011). Three clones (BS4 OTU 3) belonged to the OTU 6 cluster of *Zetaproteobacteria* (McAllister *et al.*, 2011), a phylotype closely related to Zeta OTU 2 with representatives found only at Loihi Seamount. Four clones (BS7 OTU 4) belonged to *Zetaproteobacteria* OTU 14, a relatively rare phylotype (McAllister *et al.*, 2011). No representatives were found that were in the same OTU as *M. ferrooxydans*, the stalk-forming isolate from Loihi. The overall relative abundance of *Zetaproteobacteria* clones, and detection of high numbers with the *Zetaproteobacteria*-specific FISH probe, indicate that they are prevalent in the sheath-dominated, veil-like surface layers of the mats. The absence of *Leptothrix* or other iron-oxidizing *Betaproteobacteria* provides further evidence that the sheathed

Table 3. Percent of *Zetaproteobacteria* found using different quantification methods

Method	Hiolo North (Marker 39) BS4	Upper Hiolo North (Marker 31) BS7
qPCR*	23.5%	21.2%
Clone library	36.7	29.4
FISH	54 (2.5)†	87 (3.5)†

*qPCR using Zeta-specific primers compared to bacteria-specific primers.
†% sheathed filamentous Zetas.

iron-oxidizing bacteria are most likely to be members of the *Zetaproteobacteria*. Presently, it is difficult to predict which OTU(s) might represent the sheath-forming *Zetaproteobacteria*, although it is likely to be an OTU with few sequenced clones, because even in enriched samples, sheathed cells themselves are relatively rare.

The similarity in ecology between the sheathed *Betaproteobacteria* and presumptive *Zetaproteobacteria* sheath-forming bacteria is striking. Field analyses of freshwater iron-seeps where *L. ochracea* is common indicate that it grows prolifically in the upper regions of these mats, where it is most exposed to oxygen (Emerson & Revsbech, 1994; Emerson & Weiss, 2004). Microsensor surveys have shown that microbial iron-mats at Loihi Seamount have steep oxygen gradients (Wheat *et al.*, 2000; Glazer & Rouxel, 2009) but that the surface layer is oxygenated. Those measurements were made on denser mats that did not have the surface layers described here; nonetheless, the data did indicate that the loosely adherent surface layers dominated by the sheath-forming bacteria were likely more oxygenated than the bulk mat. This indicates that sheath-forming FeOB may be more tolerant of higher ambient oxygen concentrations than is typical for other FeOB, although we have not been able to measure the oxygen concentration inside the sheath. Additionally, the sheathed bacteria could employ a similar ecological strategy as some of the sulfur bacteria by growing as mats or veils at the oxic/anoxic interface and resulting in a stabilization of the surface boundary layer and a sediment 'cap' on the diffusing anoxic waters (Jørgensen & Revsbech, 1983; Thar & Kühl, 2002; Muyzer *et al.*, 2005).

Our discovery that marine and freshwater sheath-forming FeOB are only phylogenetically distantly related represents the second case of exceptional morphological and functional similarity between marine and freshwater FeOB, despite divergent genetic backgrounds. As described in the introduction, the stalk-forming *M. ferrooxydans*, also isolated from a Loihi Seamount iron-mat, shares many morphological similarities with the freshwater, stalk-forming *Gallionella* spp. A recent detailed comparative ultrastructural analysis showed an overall conservation of traits between these two stalk-forming FeOB (e.g. cell shape, inclusions, stalk ultrastructure) with some important, yet more subtle, differences in cell surface and chemoreceptor architecture (Comolli *et al.*, 2011). Taken together, these findings suggest that effective growth on Fe (II) by FeOB in circumneutral redox boundary environments requires a unique degree of morphological and physiological specialization that has evolved separately in marine and freshwater ecosystems. The role of horizontal gene transfer or other evolutionary processes that have selected for these convergent adaptations remains to be investigated.

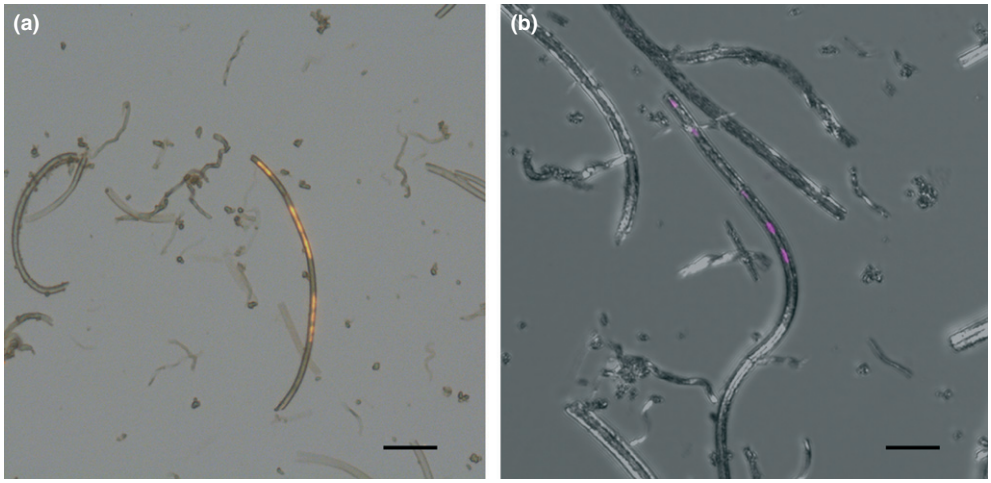

Fig. 6. Overlay of phase-contrast or DIC and florescence images showing the Zeta674 CARD-FISH probe binding to *Zetaproteobacteria* cells captured with a fluorescence microscope or a confocal microscope, a or b, respectively. Probes specific for *L. ochracea* or for *Betaproteobacteria* did not bind to cells from Loihi samples, and the Zeta674 did not bind to freshwater samples enriched in *L. ochracea* (described in McBeth *et al.*, 2013). Scale bars are 10 and 6 μm for a and b, respectively.

Acknowledgements

We thank the captain and crew of the R/V *Kilo Moana*, and pilots and operators of *Jason* II, whose work was instrumental to our success. We especially thank Jim Varnum for helping to adroitly manipulate and Geoff Wheat for helping to design the biomat syringe sampler. We thank Katrin Kießlich who helped with sample preservation during the cruise, and Debbie Powell who helped with SEM analyses. This work took place during an Iron Microbial Observatory (FeMO) expedition (2009), and we appreciate the support of Katrina Edwards and Hubert Staudigel, two other FeMO PI's. We would also like to thank three anonymous reviewers for their suggestions that have improved this manuscript. This work was supported through the NSF Microbial Observatory program through grant numbers MCB-0348330 (D.E.), MCB-0348734 (C.L.M.), and MCB-0348668/0742010 (B.M.T.). D.E. and E.F. also recieved funding from NASA EPSCoR.

References

Amann R, Krumholz L & Stahl D (1990) Fluorescent-oligonucleotide probing of whole cells for determinative, phylogenetic, and environmental studies in microbiology. *J Bacteriol* **172**: 762.

Ashelford KE, Chuzhanova NA, Fry JC, Jones AJ & Weightman AJ (2005) At least 1 in 20 16S rRNA sequence records currently held in public repositories is estimated to contain substantial anomalies. *Appl Environ Microbiol* **71**: 7724–7736.

Ashelford K, Chuzhanova N, Fry J, Jones A & Weightman A (2006) New screening software shows that most recent large 16S rRNA gene clone libraries contain chimeras. *Appl Environ Microbiol* **72**: 5734–5741.

Chan C, Fakra S, Emerson D, Fleming EJ & Edwards K (2011) Lithotrophic iron-oxidizing bacteria produce organic stalks to control mineral growth: implications for biosignature formation. *ISME J* **5**: 717–727.

Comolli L, Luef B & Chan C (2011) High-resolution 2D and 3D cryo-tem reveals structural adaptations of two stalk-forming bacteria to an iron-oxidizing lifestyle. *Environ Microbiol* **13**: 2915–2929.

Davis RE & Moyer CL (2008) Extreme spatial and temporal variability of hydrothermal microbial mat communities along the Mariana Island arc and southern Mariana Back-arc-system. *J Geophys Res* **113**: 17.

Edwards KJ, Glazer BT, Rouxel OJ *et al.* (2011) Ultra-diffuse hydrothermal venting supports iron-oxidizing bacteria and massive umber deposition at 5000 m off Hawaii. *ISME J* **5**: 1748–1758.

Emerson D & Moyer CL (2002) Neutrophilic iron-oxidizing bacteria are abundant at the Loihi seamount hydrothermal vents and play a major role in Fe oxide deposition. *Appl Environ Microbiol* **68**: 3085–3093.

Emerson D & Moyer CL (2010) Microbiology of seamounts; common patterns observed in community structure. *Oceanography* **23**: 148–163.

Emerson D & Revsbech NP (1994) Investigation of an iron-oxidizing microbial mat community located near Aarhus, Denmark: field studies. *Appl Environ Microbiol* **60**: 4022–4031.

Emerson D & Weiss JV (2004) Bacterial iron oxidation in circumneutral freshwater habitats: findings from the field and the laboratory. *Geomicrobiol J* **21**: 405–414.

Emerson D, Rentz JA, Lilburn TG & Davis RE (2007) A novel lineage of proteobacteria involved in formation of marine iron-oxidizing microbial mat communities. *PLoS ONE* **2**: e667.

Emerson D, Fleming E & McBeth J (2010) Iron-oxidizing bacteria: an environmental and genomic perspective. *Annu Rev Microbiol* **64**: 561–683.

Fleming EJ, Langdon A, Martinez-Garcia M, Stepanauskas R, Poulton N, Masland E & Emerson D (2011) What's new is old: resolving the identity of *Leptothrix ochracea* using single cell genomics, pyrosequencing and FISH. *PLoS ONE* **6**: e17769.

Forget NL, Murdock SA & Juniper SK (2010) Bacterial diversity in Fe-rich hydrothermal sediments at two south Tonga arc submarine volcanoes. *Geobiology* **8**: 417–432.

Fuchs BM, Glöckner FO, Wulf J & Amann R (2000) Unlabeled helper oligonucleotides increase the *in situ* accessibility to 16S rRNA of fluorescently labeled oligonucleotide probes. *Appl Environ Microbiol* **66**: 3603–3607.

Garcia M, Caplan-Auerbach J, De Carlo E, Kurz MD & Becker N (2006) Geology, geochemistry and earthquake history of Lõ'ihi seamount, Hawaìi's youngest volcano. *Chem Erde* **66**: 81–108.

Ghiorse W (1984) Biology of iron-and manganese-depositing bacteria. *Annu Rev Microbiol* **38**: 515–550.

Glazer B & Rouxel O (2009) Redox speciation and distribution within diverse iron-dominated microbial habitats at Lõ'ihi seamount. *Geomicrobiol J* **26**: 606–622.

Handley KM, Boothman C, Mills RA, Pancost RD & Lloyd JR (2010) Functional diversity of bacteria in a ferruginous hydrothermal sediment. *ISME J* **4**: 1193–1205.

Hodges TW & Olson JB (2009) Molecular comparison of bacterial communities within iron-containing flocculent mats associated with submarine volcanoes along the Kermadec Arc. *Appl Environ Microbiol* **75**: 1650–1657.

James RE, Scott SD, Fortin D, Clark ID & Ferris FG (2012) Regulation of Fe^{3+}-oxide Formation Among Fe^{2+}-oxidizing Bacteria. *Geomicrobiol J* **29**: 537–543.

Jørgensen BB & Revsbech NP (1983) Colorless sulfur bacteria, *Beggiatoa* spp. and *Thiovulum* spp., in O_2 and H_2S microgradients. *Appl Environ Microbiol* **45**: 1261–1270.

Karl DM, Brittain AM & Tilbrook BD (1989) Hydrothermal and microbial processes at Loihi seamount. a mid-plate hot-spot volcano. *Deep-Sea Res* **36**: 1655–1673.

Kato S, Kobayashi C, Kakegawa T & Yamagishi A (2009) Microbial communities in iron-silica-rich microbial mats at deep-sea hydrothermal fields of the southern Mariana trough. *Environ Microbiol* **11**: 2094–2111.

Kormas KA, Tivey MK, Von Damm K & Teske A (2006) Bacterial and archaeal phylotypes associated with distinct

mineralogical layers of a white smoker spire from a deep-sea hydrothermal vent site (9°N, East Pacific Rise). *Environ Microbiol* **8**: 909–920.

Lane DJ (1991) 16S/23S rRNA sequencing. *Nucleic Acid Techniques in Bacterial Systematics* (Steckebrandt E & Goodfellow M, eds), pp. 115–176. John Wiley & Sons Ltd, New York, NY.

Li J, Zhou H, Peng X, Wu Z, Chen S & Fang J (2012) Microbial diversity and biomineralization in low-temperature hydrothermal iron-silica-rich precipitates of the Lau basin hydrothermal field. *FEMS Microbiol Ecol* **81**: 205–216.

Ludwig W, Strunk O, Westram R *et al.* (2004) ARB: a software environment for sequence data. *Nucleic Acids Res* **32**: 1363–1371.

McAllister S, Davis RE, McBeth J, Tebo B, Emerson D & Moyer CL (2011) Biodiversity and emerging biogeography of the neutrophilic iron-oxidizing zetaproteobacteria. *Appl Environ Microbiol* **77**: 5445–5457.

McBeth J, Little BJ, Ray RI, Farrar KM & Emerson D (2011) Neutrophilic iron-oxidizing "Zetaproteobacteria" and mild steel corrosion in nearshore marine environments. *Appl Environ Microbiol* **77**: 1405–1412.

McBeth JM, Fleming EJ & Emerson D (2013) The transition from freshwater to marine iron-oxidizing bacterial lineages along a salinity gradient on the Sheepscot River, Maine USA. *Environ Microbiol Rep*, doi: 10.1111/1758-2229.12033.

Meyer-Dombard D, Arcy R, Amend JP & Osborn MR (2012) Microbial diversity and potential for arsenic and iron biogeochemical cycling at an arsenic rich, shallow-sea hydrothermal vent (Tutum bay, Papua New Guinea). *Chem Geol*, doi: 10.1016/j.chemgeo.2012.02.024.

Moyer CL, Dobbs FC & Karl DM (1995) Phylogenetic diversity of the bacterial community from a microbial mat at an active, hydrothermal vent system, Loihi seamount, Hawaii. *Appl Environ Microbiol* **61**: 1555–1562.

Muyzer G, Yildirim E, van Dongen U, Kühl M & Thar R (2005) Identification of '*Candidatus Thioturbo danicus*', a microaerophilic bacterium that builds conspicuous veils on sulfidic sediments. *Appl Environ Microbiol* **71**: 8929–8933.

Neubauer SC, Emerson D & Megonigal JP (2002) Life at the entergetic edge:kinetics of circumneutral iron oxidation by lithotrophic iron-oxidizing bacteria isolate from the wetland-plant rhizosphere. *Appl Environ Microbiol* **68**: 3988–3995.

Pernthaler A, Pernthaler J & Amann R (2002) Fluorescence *in situ* hybridization and catalyzed reporter deposition for the identification of marine bacteria. *Appl Environ Microbiol* **68**: 3094–3101.

Pruesse E, Quast C, Knittel K, Fuchs BM, Ludwig W, Peplies J & Glöckner FO (2007) SILVA: a comprehensive online resource for quality checked and aligned ribosomal RNA sequence data compatible with ARB. *Nucleic Acids Res* **35**: 7188–7196.

Rasband W (2004) *ImageJ: Image Processing and Analysis in Java*. http://rsb.info.nih.gov/ij/.

Rassa AC, McAllister SM, Safran S & Moyer CL (2009) Zetaproteobacteria dominate the formation of microbial mats in low-temperature vents at Loihi seamount, Hawaii. *Geomicrobiol J* **26**: 623–638.

Ruby EG, Wirsen CO & Jannasch HW (1981) Chemolithotrophic sulfur-oxidizing bacteria from the Galapagos rift hydrothermal vents. *Appl Environ Microbiol* **42**: 317–324.

Singer E, Emerson D, Webb EA *et al.* (2011) *Mariprofundus ferrooxydans* pv-1 the first genome of a marine Fe(II) oxidizing Zetaproteobacterium. *PLoS ONE* **6**: e25386.

Spring S, Jackel U, Wagner M & Kampfer P (2004) *Ottowia thiooxydans* gen. nov, sp nov, a novel facultatively anaerobic, N_2O-producing bacterium isolated from activated sludge, and transfer of *Aquaspirillum gracile* to *Hylemonella gracilis* gen nov, comb nov. *Int J Syst Evol Microbiol* **54**: 99–106.

Tartof KD & Hobbs CA (1987) Improved media for growing plasmid and cosmid clones. *Bethesda Res Lab Focus* **9**: 12.

Teske A & Stahl D (2002) Microbial mats and biofilm: evolution, structure and function of fixed microbial communities. *Biodiversity of Microbial Life* (Staley JT & Reysenbach AL, eds), pp. 49–100. Wiley-Liss, New York, NY.

Thar R & Kühl M (2002) Conspicuous veils formed by vibrioid bacteria on sulfidic marine sediment. *Appl Environ Microbiol* **68**: 6310–6320.

Toner BM, Berquó TS, Michel FM, Sorensen JV, Templeton AS & Edwards KJ (2012) Minerology of iron microbial mats from Loihi Seamount. *Front Microbiol* **3**: 1–18.

Wallner G, Amann R & Beisker W (1993) Optimizing fluorescent in situ hybridization with rRNA-targeted oligonucleotide probes for flow cytometric identification of microorganisms. *Cytometry* **14**: 136–143.

Wankel SD, Germanovich L, Lilley MD, Genc G, Diperna CJ, Bradley AS, Olson EJ & Girguis PR (2011) Geochemical flux and metabolic activity associated with the hydrothermal subsurface. *Nat Geosci* **4**: 461–468.

Wheat CG, Jannasch HW, Plant JN, Moyer C, Sansone FJ & McMurtry GM (2000) Continuous sampling of hydrothermal fluids from Loihi seamount after the 1996 event. *J Geophys Res* **105**: 19353–19367.

Supporting Information

Additional Supporting Information may be found in the online version of this article:

Fig. S1. Electron Dispersive X-Ray Spectra for (A) sheaths from Loihi seamount and (B) freshwater sheaths. Sheaths regions outlined in green (present in insets) were used for spectra analysis.

Data S1. Additional materials and methods used in this study.

Table S1. Probes and Primers used in this study.